Journal of Power Sources 190 (2009) 285–292

Contents lists available at ScienceDirect

Journal of Power Sources

journal homepage: www.elsevier.com/locate/jpowsour

Anionic polysulfone ionomers and membranes containing fluorenyl groups for anionic fuel cells

Junfeng Zhou, Murat Unlu, Jose A. Vega, Paul A. Kohl*

Chemical and Biomolecular Engineering, Georgia Institute of Technology, Atlanta, Georgia 30332-0100, USA

ARTICLE INFO

Article history:
Received 24 October 2008
Received in revised form 27 December 2008
Accepted 30 December 2008
Available online 14 January 2009

Keywords:
Anion exchange membrane
Carbonate fuel cell
Conductivity

ABSTRACT

Poly(arylene ether sulfone) ionomers containing fluorenyl groups and functionalized with benzyltrimethylammonium groups were synthesized through polycondensation, chloromethylation, and amination reactions. The resulting polymers were characterized by ^{1}H NMR, FT-IR and TGA. Polymer membranes were solvent cast from DMF on Teflon plates to form clear, flexible anion exchange membranes (AEMs). Carbonate anions had conductivities in the AEMs up to 63.12 mS cm^{-1} at 70 °C and were used in a carbonate fuel cell. The membranes were stable in 1 M carbonate solution (pH 11). However, conductivity loss was observed during soaking in 1 M hydroxide solution (pH > 14) at 50 °C. A carbonate fuel cell operating at room temperature with H_2 at the anode and O_2 and CO_2 at the cathode had a maximum power density of 4.1 mW cm^{-2}.

1. Introduction

Fuel cells can be used in transportation, portable electronics, and stationary applications because of their high efficiencies and low pollution levels [1–3]. Polymer electrolyte fuel cells operating at moderate temperature are currently being developed and are promising candidates for a wide range of applications [4–5]. In particular, fuel cells using proton exchange polymer membranes (PEMs) are important because they can be used near room temperature [6–7]. Unfortunately, there are numerous obstacles that impede commercial development, such as complex water management, limited lifetime due to membrane and electrode degradation, costly metal catalysts, perfluorinated polymer membranes for stability, CO poisoning of electrode catalyst, and slow oxygen reduction kinetics [8–12]. Anionic fuel cells can potentially address many of the shortcomings of PEM fuel cells. The PEM electrolyte can be replaced by an anion exchange membrane (AEM) allowing hydroxide or other anions to be used. There is current research exploring novel AEMs that conduct hydroxide as alternative PEM candidates [13–15].

To date, AEMs based on quaternized polymers have been reported for use in anionic fuel cells, such as blending materials containing quarternary ammnonium groups [16], aminated poly(oxyethylene) methacrylates, quaternized polyethersulfone cardo [17], radiation-grafted poly(vinylidene fluoride) (PVDF) [18], poly(tetrafluoroethene-co-hexafluropropylene) (FEP) [19], quaternized crosslinked poly(vinyl alcohol) (PVA) [20], quaternized poly(phthalazinon ether sulfone ketone) [21], and aminated poly(phenylene) [22]. Among these materials, aromatic polymers are the preferred candidates for fuel cell applications due to their excellent thermal and mechanical properties as well as their resistance to oxidation and stability in acidic and alkaline conditions [23,24]. However, the stability of the fixed cationic site in alkaline conditions is a concern due to nucleophilic attack by anions. If fluorenyl groups are introduced into the polymer backbone, the AEM may retain its ionic conductivity and durability in alkaline fuel cell applications [25]. In this study, partially fluorinated, polyaromatic-based condensation polymers containing quaternary ammonium groups are reported.

Anionic fuel cells generally use hydroxide as the conductive anion. Although the high conductivity of hydroxide is attractive, hydroxide is an extremely aggressive nucleophile and can degrade the quaternary ammonium cations on the polymer, especially at high temperature [26]. Nucleophilic attack of the cation site on polymeric AEMs is a major obstacle to achieve long term stability. Lowering the alkalinity of the mobile anion could mitigate nucleophic degradation [27].

In this study, a series of novel poly(arylene ether sulfone) polymers containing fluorenyl groups and functionalized with benzyltrimethylammonium groups was synthesized through polycondensation, chloromethylation, and amination reactions. Carbonate ion conductivity in the AEMs was evaluated. A membrane electrode assembly (MEA) was fabricated and used in a hydrogen fuel cell operating on the carbonate cycle.

* Corresponding author.
E-mail address: Paul.kohl@chbe.gatech.edu (P.A. Kohl).

0378-7753/$ – see front matter © 2009 Elsevier B.V. All rights reserved.
doi:10.1016/j.jpowsour.2008.12.127

2. Experimental

2.1. Materials

Bis(4-fluorophenyl) sulphone (FPS) (Alfa Aesar Co., Inc.), 1,1,2,2-tetrachloroethane (Alfa Aesar Co., Inc.), 4,4'-(hexafluoroisopropylidene)diphenol (6F-BPA) (Alfa Aesar Co., Inc.), toluene (Alfa Aesar Co., Inc.), chloromethyl methyl ether (Aldrich Co., Inc), tin(IV) chloride (Alfa Aesar Co., Inc.) and trimethylamine (Alfa Aesar Co., Inc.) were used as received. *N*,*N*-Dimethylacetamide (DMAc) (Alfa Aesar Co., Inc.) was dried over 3-A molecular sieves prior to use. Potassium carbonate (Aldrich Co., Inc.) was dried at 120 °C for 24 h before polymerization. Other chemicals were of commercially available grade and used as received.

2.2. Synthesis of poly(arylene ether sulfone) (PSF) [28,29]

The synthesis procedure of poly(arylene ether sulfone) is as follows. A 250 mL three-necked round-bottomed flask equipped with a magnetic stirring bar, a N_2 inlet, and an addition funnel, was charged with FPS (0.05 mol, 12.7125 g), 6F-BPA (0.05 mol, 16.8115 g), potassium carbonate (0.125 mol, 17.2768 g), toluene (50 mL) and DMAc (125 mL). The mixture was stirred at room temperature for 20 min and then heated at 140 °C for 3 h and at 165 °C for 5 h under N_2 atmosphere. After the reaction, the solution was poured dropwise into deionized water (3 L) and a white product was precipitated from the solution. After being washed with hot deionized water and ethanol several times, the resulting product was dried under vacuum at 60 °C for 15 h.

2.3. Preparation of chloromethylated poly(arylene ether sulfone) (CMPSF) [30–32]

The chloromethylation procedure of poly(arylene ether sulfone) is as follows. The chloromethylation reaction was performed in a glass flask heated in an oil bath and equipped with a magnetic stirring bar, a N_2 inlet and a reflux condenser. PSF (4.9093 g) was dissolved in 1,1,2,2-tetrachloroethane (218.1802 g, 137.22 mL) solvent, then a mixture of chloromethyl methyl ether (0.1782 mol, 13.54 mL) and $SnCl_4$ (2.74 mmol, 0.7125 g) was slowly added to the above solution. The reaction was heated at 120 °C for 3 days. After cooling to room temperature, the mixture was poured into ethanol (2 L). The precipitate was collected by filtration, dried under vacuum, then dissolved in 100 mL THF, and reprecipitated into ethanol (2 L) to further remove unreacted materials and solvent. The precipitate was collected by filtration and dried under vacuum to yield an off-white solid.

2.4. Preparation of poly(arylene ether sulfone) functionalized with benzyltrimethylammonium groups (QAPSF)[33]

The chloromethylated poly(arylene ether sulfone) was submerged in a 45% (w/w) solution of trimethylamine in water and the mixture was stirred for 48 h at room temperature. During the reaction, CMPSF would gradually be dissolved in the solution. After the reaction, the mixture was poured into an evaporating dish for dry at room temperature in order to remove trimethylamine and water.

2.5. Preparation of ammonium based membrane for carbonate fuel cell

QAPSF was dissolved in dimethylformamide (DMF) to make a 6.0 wt% solution. The solution was filtered to remove small particles and cast on Telfon plates. The films were dried at room temperature for 12 h. The membranes were about 100 μm thick and were further dried under vaccum at 75 °C for 15 h. The anion exchange membranes were stored in the Cl^- form, later converted to the carbonate form prior to use.

Conversion from the chloride form to the carbonate form occurred within one day of use. The AEM was soaked in a 1 M aqueous sodium carbonate. The sodium carbonate solution was changed several times with a fresh solutions during a 2-h period to ensure substantial ion exchange. The resulting membrane was then soaked in water for 1 h with at least two changes of water to remove excess sodium carbonate.

2.6. Membrane characterization

The ^1H NMR spectra of the synthesized polymers was recorded for structural characterization. Data were collected with a Model DMX400 spectrometer using chloroform-d solutions. FT-IR absorption spectra were recorded using a Nicolet Magna 560 FT-IR spectrometer. The FT-IR samples were made by casting films on KBr tablets from a DMF solution. The samples were then analyzed in transmission mode.

Thermogravimetry analysis (TGA) was carried out in flowing nitrogen (60 $cm^3\ min^{-1}$) using a TA Q50 thermal analyzer. Samples were heated from ambient temperature to 800 °C at a heating rate of 5 °C min^{-1}.

The water uptake of the samples was analyzed by first drying the films in a desiccators over anhydrous calcium chloride at ambient temperature until a constant dry weight (W_d) was obtained [34]. The dry membranes were immersed in deionized water at different temperatures for 24 h. The surface water was swabbed away with tissue paper before weighing. The weights were measured several times until a constant weight (W_w) was achieved. The water uptake of membranes was calculated using the following formula:

$$\text{Water uptake } (\%) = \left[\frac{(W_w - W_d)}{W_d}\right] \times 100\% \quad (1)$$

where W_d and W_w are the weight of dried and wet samples, respectively.

The ionic conductivity of the membranes was measured by a four-electrode ac impedance method using a frequency response analyzer including potentiostat/galvanostat (PAR 2273, Princeton Applied Research) from 1 Hz to 2 MHz. All membranes in the carbonate form were initially hydrated by immersing in deionized water for 24 h at room temperature before measuring the conductivity. The resistance of the 1 M Na_2CO_3 solution ($R_{solution}$) was measured without the membrane present in a glass conductivity cell. Then, the fully hydrated membrane was placed in the middle of the conductivity glass cell and the resistance (R_{total}) of the solution with membrane was measured. The membrane resistance (R) was obtained from the difference between the measured resistances ($R_{solution}$ and R_{total}). Conductivity measurements were carried out from 25 to 80 °C. Conductivity measurements were carried out from 25 to 80 °C. The conductivity (σ) of the membranes was calculated using the following equation:

$$\sigma = \frac{L}{RA} \quad (2)$$

where L, R, and A denote the thickness of the membrane, the membrane resistance, and the cross-sectional area of the membrane, respectively.

The fuel cell tests were performed by fabricating electrodes on the AEMs using commercial carbon-supported platinum (Pt/C) catalysts with 20% Pt (E-Tek). The catalyst inks were prepared by sonicating a mixture of catalyst powders and ionomer in a solvent mixture of dimethylformamide and water. The catalyst slurry was paint on Toray carbon paper (TGPH-090) and dried at room temperature. The catalyst and ionomer loadings were 1 and 0.8 mg cm^{-2},

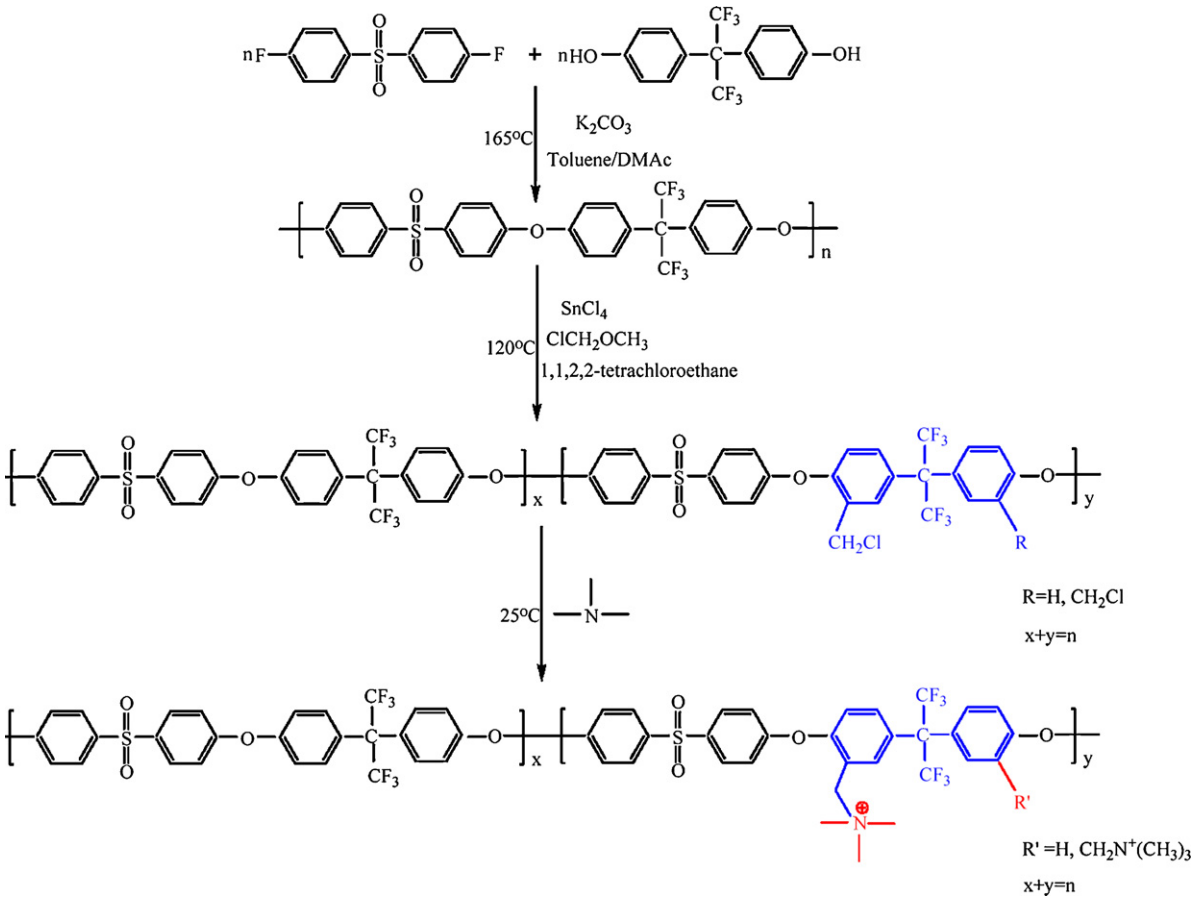

Scheme 1. Synthesis procedure of novel polysulfone-anion exchange membrane.

respectively. The electrodes were pressed onto the AEMs at room temperature for 5 min. Once the MEAs were assembled, they were soaked in 0.5 M Na_2CO_3 solution for 5 h to exchange the chloride ions in the ionomers with carbonate ions. All MEAs were preconditioned by steady state operation at 600 mV for at least 24 h before collecting polarization curves. Electrochemical measurements were performed using a PAR 2273 potentiostat/galvanostat. The fuel cell tests were conducted at 25 °C at ambient pressure.

3. Results and discussion

3.1. Synthesis and characterization of the polymers

Poly(arylene ether sulfone) was first synthesized through a polycondensation reaction. The copolymerization of 6F-BPA and FPS was carried out in DMAc/toluene cosolvent in a nitrogen ambient. Toluene was used to dehydrate the reaction mixture. The reaction temperature was controlled at 140 °C to remove the water generated during the bisphenoxide formation, and then increased slowly to carry out the copolymerization. The chloromethylated polysulfone was prepared by Friedel–Crafts electrophilic substitution reaction under anhydrous conditions at 120 °C using PSF as the original material, 1,1,2,2-tetrachloroethane as the solvent, chloromethyl methyl ether as the chloromethyl reagent, and anhydrous $SnCl_4$ as the catalyst. In order to avoid crosslinking resulting from methylene bridges between macromolecular chains [32], the chloromethylation was performed at dilute conditions with little catalyst. The chloromethyl substitute was transformed into the quaternary amino base by immersing the polymers in a solution consisting of 45% trimethylamine solution at room temperature for 2 days. The synthetic scheme for the preparation of poly(arylene ether sulfone) containing fluorenyl groups and functionalized with benzyltrimethylammonium groups is shown in Scheme 1.

The chemical structures of the neat PSF and CMPSF were investigated by liquid phase ^{1}H NMR spectroscopy with $CDCl_3$ as the solvent and reference. As shown in Fig. 1A, the aromatic region of PSF is divided into three sections: a high-field (7.00–7.10 ppm), mid-field (7.30–7.40 ppm), and low-field (7.85–7.95 ppm). The peak heights for these regions are 2H:1H:1H, reflecting the chemical structure of the PSF repeat unit. The high-field signals have the characteristic chemical shift of aromatic hydrogen atoms at the position of an electron-rich, ether linkage. The middle-field signals are ascribed to the aromatic hydrogen atoms close to the fluorinated bonds. The low-field signals are assigned to the aromatic hydrogen atoms near the sulfone groups. The ^{1}H NMR result is thus consistent with the structure of the copolymer PSF. Compared with the ^{1}H NMR spectrum of PSF in Fig. 1A, the characteristic peaks of $-CH_2Cl$ corresponding to the newly formed chloromethyl group can be seen at δ = 4.583 and 4.699 (h) in Fig. 1B. Moreover, the peaks for the protons in the diphenyl units (a and b) decrease in size, and three new peaks of equal intensity (e, f and g) appear in the aryl region. These peaks confirm the successful preparation of the chloromethylated copolymer CMPSF [35].

The degree of chloromethylation of CMPSF is calculated from the ^{1}H NMR spectra where the peak areas from the chloromethyl groups are compared to the peak areas for all the aromatic protons. As shown in Table 1, the chloromethylated PSFs possess 1.24 and 1.50 chloromethyl groups in each repeat unit at various reaction conditions. Obviously, the degree of chloromethylation strongly depended on the reaction time.

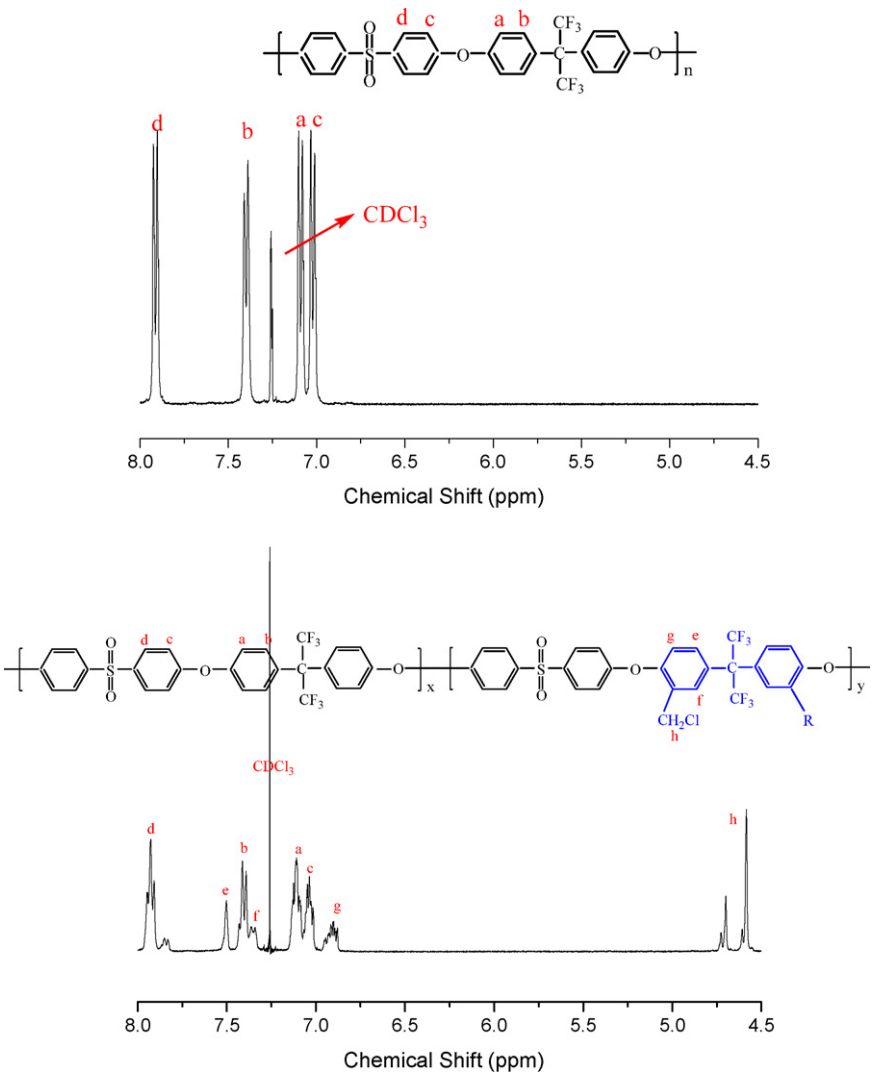

Fig. 1. ^{1}H NMR spectra of PSF (A) and CMPSF (B).

The chemical structures of these copolymers were further investigated by FT-IR. The FT-IR absorption spectra of PSF, CMPSF, and QAPSF are shown in Fig. 2. As shown in Fig. 2A, the characteristic absorption peak at 3028 cm^{-1} is due to the aromatic C–H stretch. The sharp absorption bands at 1587, 1509, and 1489 cm^{-1} are due to the skeletal vibration of the aromatic hydrocarbons. The peak at 1246 cm^{-1} is assigned to the antisymmetric vibration of the ether linkage. The characteristic absorption bands at 1205 and 1020 cm^{-1} are from the symmetric and asymmetric stretching vibration of the S=O bond. Comparing Fig. 2A with Fig. 2B (the spectrum of CMPSF), as well as the characteristic absorption bands for PSF, it is found that the intensity of the absorption band at 732 cm^{-1} has increased, which is due to the introduction of chloromethyl groups. This shows that CMPSF was successfully prepared after the PSF underwent a Friedel–Crafts reaction [32].

Table 1
Chloromethylation reaction conditions and the degree of chloromethylation (DC).

Sample	n ($ClCH_2OCH_3$) Equivalents of PSF unit	Time (days)	DC[a]
CMPSF-1	20	3	1.24
CMPSF-2	20	5	1.50

[a] Degree of chloromethylation = number of chloromethyl groups/repeat unit, calculated from ^{1}H NMR spectra.

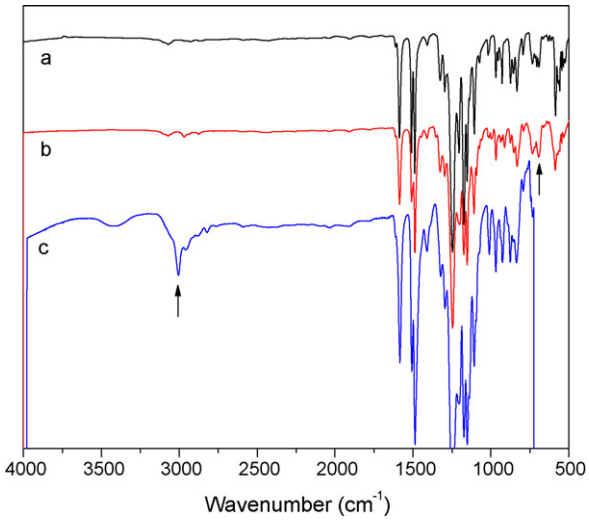

Fig. 2. FT-IR spectra of PSF (A), CMPSF (B) and QAPSF (C).

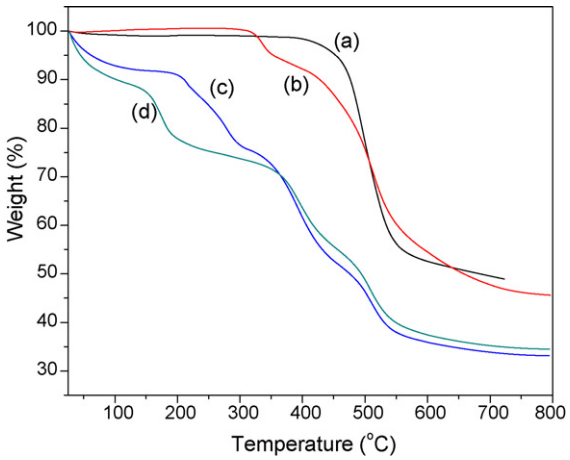

Fig. 3. Typical TGA curves of the polymers under nitrogen atmosphere: (A) PSF, (B) CMPSF, (C) QAPSF in chloride, and (D) QAPSF in carbonate.

Since QAPSF cannot be dissolved in chloroform-d, the successful introduction of the quaternary ammonium groups of the copolymers was confirmed by FT-IR. The differences between the CMPSF and QAPSF spectra can be seen in Fig. 2B and C. In addition to the characteristic absorption band at 3005 cm^{-1} for the $-CH_3$ stretch, which is due to the introduction of the trimethyl groups, the characteristic absorption peak of $N-CH_2$ at 1421 cm^{-1} appears in Fig. 2C. The results show that the quaternary ammonium groups were indeed attached to the copolymers.

3.2. Thermal stability and solubility

The thermal stability of the polymer is a key metric to forming ionic conducting ionomers for use in a fuel cell. Fuel cell performance generally improves at elevated temperature. Operation between 40 and 120 °C is of interest. Thermogravimetric analysis was carried out on the polymers synthesized here to examine their thermal stability. The TGA curves for PSF, CMPSF and QAPSF are shown in Fig. 3. The 5% weight loss temperature for the neat PSF is 455 °C, as shown in Fig. 3A. PSF is thermally stable because of its rigid aromatic structure. Two decomposition steps are observed in the TGA for CMPSF (Fig. 3B). The first degradation step, from 311 to 350 °C, is attributed to the loss of chloromethyl groups. The second decomposition step, beginning at about 450 °C, corresponds to the degradation of the PSF backbone. The pendent quaternary ammonium groups have a great influence on the CMPSF thermal property. The TGA curves for QAPSF in chloride and carbonate forms are shown in Fig. 3C and D, respectively. The initial weight loss of QAPSF in chloride from 25 to 220 °C is attributed to loss of residual solvent (DMF) and water. The second weight loss above 200 °C is due to cleavage of the quaternary ammonium groups from QAPSF. The third weight at temperatures greater than 380 °C is due to the degradation of the polymer backbone. Comparing Fig. 3C and D, it is found that the decomposition of QAPSF in the chloride and carbonate forms is similar. However, the decomposition temperature of the quaternary ammonium groups of QAPSF with carbonate anions is at about 150 °C. This shows that quaternary ammonium groups are less stable in dry, alkaline condition. In addition, it is interesting to note that the dehydration of QAPSF continues well above 100 °C indicating strong hydrogen bonding of water to the amine [36].

The solubility of the polymers was investigated by dissolving 0.05 g polymers in 5 mL solvent. Table 2 shows the solubilities of PSF, CMPSF and QAPSF in several solvents. It can be seen that PSF and CMPSF are soluble in polar, aprotic solvents (such as DMF and DMAc) and chloridized solvents (such as chloroform and 1,1,2,2-tetrachloroethane). They are insoluble in some protic solvents such as water and ethanol. However, after the attachment of the quaternary ammonium groups, QAPAF is soluble or swells in water and ethanol because of the hydrophilic quarternary ammonium groups. It is noted that the solubility of QAPSF strongly depends on the degree of chloromethylation. Excessive chloromethylation should be avoided when the AEM is used in a liquid methanol fuel cell.

Table 2
The solubility of PSF, CMPSF and QAPSF in different solvents.

Solvent	PSF	CMPSF	QAPSF
Water	I	I	SW
Ethanol	I	I	SW or S
Chloroform	S	S	I
Tetrahydrofuran	S	S	I
N,*N*-Dimethylformamdie	S	S	S
N,*N*-Dimethylacetamide	S	S	S

S: soluble; I: insoluble; SW: swelling.

3.3. Durability of QAPSF membranes in hydroxide and carbonate solution

The durability of the fixed cationic charge on the polymer is critical for its use as an AEM in anionic fuel cell applications. To explore the durability of the QAPSF membranes in different pH solutions, the ionic conductivity of these membranes was evaluated at 50 °C as a function of time (Fig. 4). It was found that the conductivity of the QAPAS membrane in hydroxide gradually decreases from 36.12 to 2.45 mS cm^{-1} within 80 h, whereas the QAPSF membrane in carbonate still retains good conductivity and strength for over 80 h. This is reasonable when considering the rate of nucleophic attack at the different pH conditions. Hydroxide is an extremely aggressive nucleophile and degrades the quaternary ammonium cation on the polymer, especially at high temperature, compared to the lower pH carbonate solution [37]. The ability to operate anionic fuel cells at pH values between 10 and 12 is desirable because hydroxide attack of the fixed cation occurs to a lesser extent allowing for longer fuel cell life.

3.4. Water uptake

Water uptake is known to have a profound effect on the membrane conductivity and mechanical properties [38]. Adequate water loading is needed to maintain good ionic conductivity; however, excessive water uptake results in membrane swelling and loss of dimensional stability. Here, we characterized the water uptake capacity by measuring the water content of these membranes in

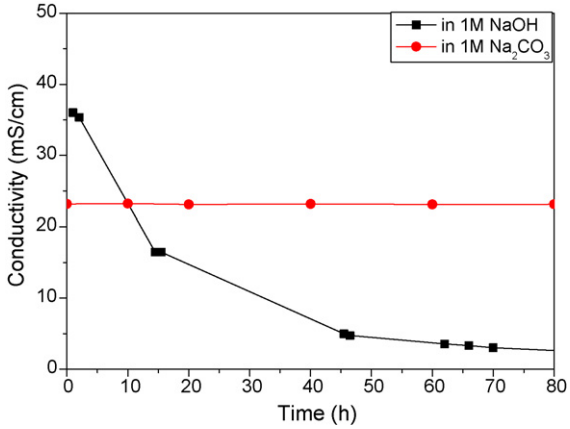

Fig. 4. Durability of the ionic conductivity of the QAPSF membranes at 50 °C in 1 M NaOH (A) or Na_2CO_3 (B) solution.

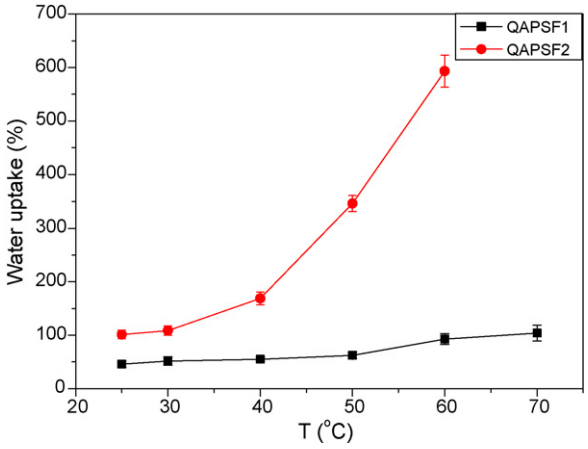

Fig. 5. Temperature dependence of water uptake of the QAPSF membranes.

the carbonate form at different temperatures. Fig. 5 shows that the water uptake of the QAPSF membranes in the carbonate form increases with the degree of chloromethylation and temperature. This is because the higher degree of chloromethylation and temperature will result in higher hydrophilicity from the quaternary ammonium groups. It is noted that the QAPSF2 membrane with the higher degree of chloromethylation had considerable swelling, resulting in poor mechanical strength at high temperature. At 80 °C, the membrane dissolved in the water after 24 h. Thus, there is an optimum degree of chloromethylation for the membranes when used in a polymer electrolyte fuel cell at >50 °C.

3.5. Ionic conductivity and activation energy

The membranes in the carbonate form were initially hydrated by immersion in deionized water for 24 h at room temperature before the ionic conductivity measurements. The ionic conductivity of the membranes in the carbonate form as a function of the temperature is shown in Fig. 6. The ionic conductivity of these membranes increases with the degree of chloromethylation and temperature. The conductivity of the two membranes (QAPSF1 and QAPSF2) is 10 mS cm^{-1} at 25 °C and increases to over 60 mS cm^{-1} at higher temperature. This is desirable when uses as an anion exchange membrane in a fuel cell. The high conductivity is a result of high level of hydration and greater ion mobility. The conductive channels formed by microphase separation create conductive channels in the AEM. However, the conductivity of the QAPSF membranes drops slightly at 80 °C, which indicates that these membranes lose some

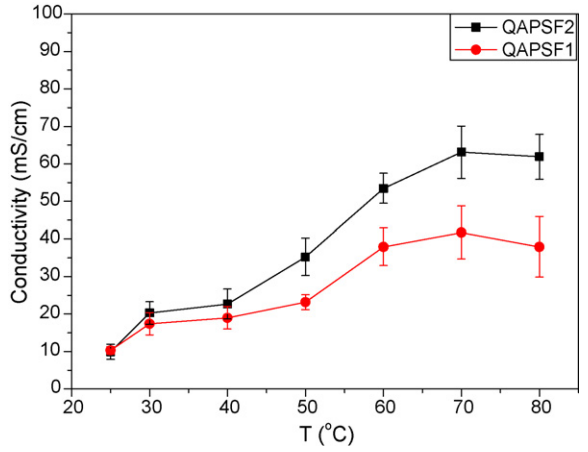

Fig. 6. Temperature dependence of the ionic conductivity of the QAPSF membranes.

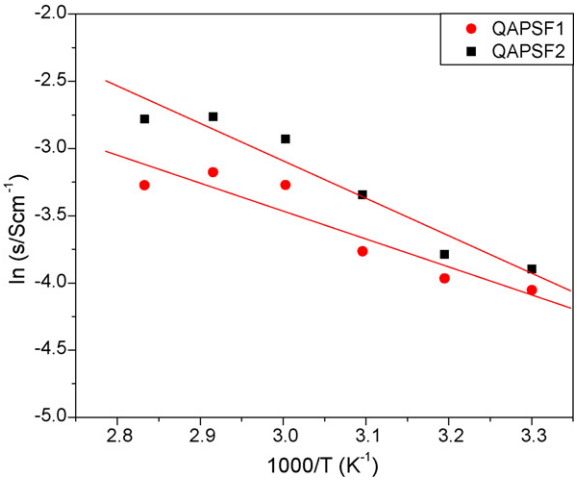

Fig. 7. The ln σ vs. 1000/T plots for the QAPSF membranes; the lines indicate the linear regression.

water. This behavior is very similar to that for proton conduction in hydrated polymer electrolytes [39].

The activation energy for ion-migration, E_a, was estimated from the linear regression of ln(conductivity) vs. 1000/T as shown in Fig. 7, assuming an Arrhenius behavior. The ion transport activation energy E_a for the QAPSF membrane was calculated using Eq. (3): [20].

$$E_a = -b \times R \quad (3)$$

where b is the slope of the line regression of ln σ (S cm^{-1}) vs. 1000/T (K^{-1}) plots, and R is the gas constant (8.31 J K^{-1} mol^{-1}).

The E_a of the QAPSF membranes are 23.03 and 43.80 kJ mol^{-1}, respectively. These values are higher than the E_a of Nafion®-115 (6.00 kJ mol^{-1}) as reported by Slade and co-worker [40]. This shows that the carbonate ion mobility in these QAPSF membranes is more sensitive to temperature than proton migration in Nafion®-115. This is likely due to the larger size of carbonate ions, as compared to hydrated protons, and the restored ionic cluster structure [19,40].

3.6. Single fuel cell performances

Membrane electrode assemblies were fabricated using QAPSF1 and QAPSF2 membranes and were tested in fuel cells using carbonate as the conducting ion. The anode stream was hydrogen with flow rate of 3 mL min^{-1}. The cathode stream was an O_2 and CO_2 mixture with flow rates of 3 and 6 mL min^{-1}, respectively. Both gas streams were 100% humidified at 25 °C and ambient pressure. The fuel cell performances are shown in Fig. 8. Maximum power density obtained was 4.1 and 3.1 mW cm^{-2} for the QAPSF2 and QAPSF1 membranes, respectively. These performances are about an order of magnitude greater than the performance of the fuel cells using commercial quaternary ammonium membranes under the same test conditions [41]. This increase in performance with the AEMs synthesized here is most likely due to the availability of solubilized ionomer so that electrode fabrication is facilitated using catalyst ink. In the previous study, the electrodes were prepared by physical compression of the catalyst onto the commercial membrane. The assemblies suffered from poor ionic conductivity between the Pt catalyst and the solid polymer membrane. The early results obtained in this study are very promising, considering the fact that the electrode composition and structure have not been optimized for this application.

In a carbonate cycle, CO_2 reacts with O_2 forming carbonate ions at the cathode (Eq. (4)). Carbonate ions migrate from the cathode to the anode through the AEM. Hydrogen is oxidized in the presence

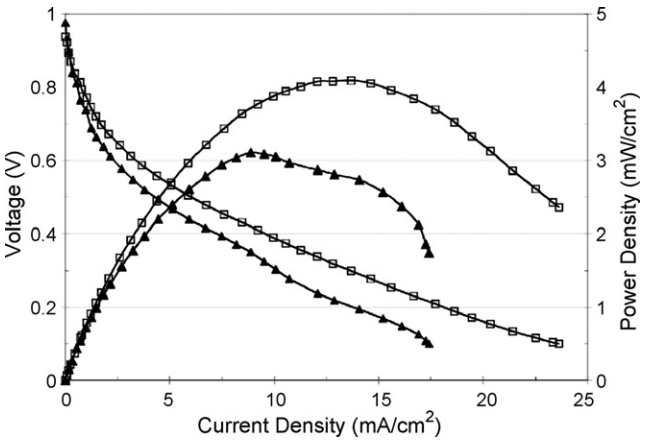

Fig. 8. Fuel cell performances of the QAPSF1 and QAPSF2 membranes at 25 °C. Anode was H_2 (6 mL min^{-1}); cathode was O_2 (3 mL min^{-1}) and CO_2 (6 mL min^{-1}).

of carbonate to produce CO_2 and H_2O at the anode, as shown in Eq. (5).

$$2CO_2 + O_2 + 4e^- \rightarrow 2CO_3^{2-} \quad (4)$$

$$H_2 + CO_3^{2-} \rightarrow H_2O + CO_2 + 6e^- \quad (5)$$

However, it is important to note that oxygen reduction can also occur by reduction of O_2 with H_2O (Eq. (6)) resulting in hydroxide formation and transport in the AEM.

$$O_2 + H_2O + 4e^- \rightarrow 4OH^- \quad (6)$$

It is of interest to distinguish between hydroxide and carbonate ion formation and migration to the anode. However, since membrane conductivity is highly dependent on water content, humidification cannot be eliminated in the control experiments.

The production and transport of carbonate, the carbonate cycle, was established by showing that CO_2 was consumed at the cathode and was produced at the anode. The consumption of CO_2 at the anode was examined by interrupting the flow of CO_2 in the cathode stream. Initially, the fuel cell was operated with the flow rates of 6, 3, and 6 mL min^{-1} for hydrogen, oxygen, and carbon dioxide, respectively. The cathode and anode streams were both humidified. Fig. 9 shows the fuel cell current at a constant voltage of 600 mV (25 °C). When the flow of CO_2 was interrupted leaving the oxygen and water flow rates the same, the current density dropped rapidly from 3.2 to 2.2 mW cm^{-2}. This large drop shows that CO_2 contributes to the reaction at the cathode. When the CO_2 flow was turned back on, the current density went back to 3.2 mA cm^{-2}. If

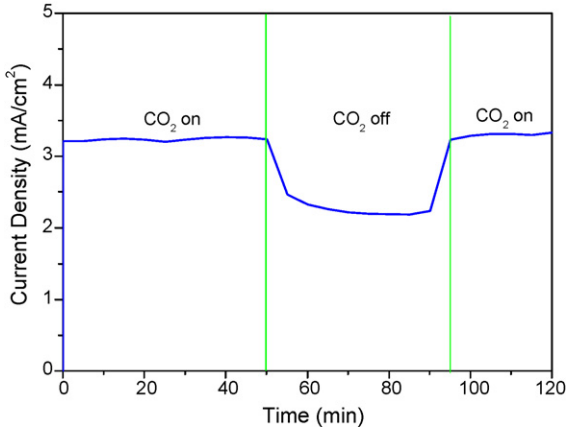

Fig. 9. Steady state operation at 600 mV on H_2 (3 mL min^{-1})/O_2 (3 mL min^{-1}) + CO_2 (6 mL min^{-1}). Both gas streams were 100% humidified. CO_2 feed was interrupted.

CO_2 were not electrochemically involved, only diluting the oxygen gas, the current would increase when the CO_2 flow was terminated because the partial pressure of oxygen and water would increase. In contrast, the addition of CO_2 to the cathode stream increases the current density.

If CO_2 were electrochemically consumed at the cathode resulting in the formation of carbonate ions which migrate to the anode, then CO_2 would be produced at the anode when hydrogen was oxidized, as shown by Eq. (5). If hydroxide was the conductive ion, only water would be produced at the anode. The production of CO_2 in the anode compartment was confirmed by flowing the anode product gas through a calcium hydroxide solution. Carbon dioxide present in the anode gas stream would then result in the precipitation of $Ca(OH)_2$. CO_2 in the anode exhaust resulted in an insoluble $CaCO_3$ precipitate. The possible diffusion of CO_2 through the membrane from the cathode stream to the anode stream was considered. Control experiments were performed to verify that the CO_2 observed in the anode stream was indeed due to the electrochemical oxidation of hydrogen in the presence of carbonate. First, the cell was operated at 4 mA cm^{-2} and 3 mL min^{-1} hydrogen flow rate at the anode and a cathode flow composed of a mixture of 3 mL min^{-1} oxygen and 6 mL min^{-1} carbon dioxide. The cell was operated long enough to ensure the anode compartment was flushed of any residual gases from start-up. The steady state composition of gas in the anode exhaust was bubbled through a 0.01 M $Ca(OH)_2$ solution. Within few seconds, a milky precipitate was observed in the $Ca(OH)_2$ solution. The amount of precipitate increased with the time as the cell operated. This test clearly shows the presence of CO_2 in the anode exhaust.

Second, the possible diffusion of CO_2 through the membrane was investigated. The control test involved using the same cell and membrane at identical conditions to the one described above except the cell current was held at zero. The anode gas was first purged to clean any residual gases by using the same gas flow rate at the anode: 3 mL min^{-1} hydrogen. The gas mixture at the cathode was again 3 mL min^{-1} oxygen and 6 mL min^{-1} carbon dioxide. The anode exhaust was then bubbled through the $Ca(OH)_2$ test solution after ensuring the anode compartment was free from ambient gas. The $Ca(OH)_2$ test solution remained clear with no precipitate. This is in contrast to results from the operating cell and shows that CO_2 diffusion through membrane from the cathode to the anode is insignificant.

The increase in fuel cell performance and production of CO_2 at the anode are clear signs that CO_2 is materially involved in the electrochemical processes and is ionically transported through the AEM. The individual contributions of carbonate and hydroxide ions in the cell operation were not evaluated. This will be studied as a function of temperature, current, and feed conditions.

4. Conclusion

A series of novel poly(arylene ether sulfone) containing fluorenyl groups and functionalized with benzyltrimethyl ammonium groups was synthesized through the polycondensation, chloromethylation, and amination reactions. QAPSF was cast from DMF solvent on Teflon plates to form clear, flexible AEMs. The carbonate ions in the AEMs exhibited excellent conductivities up to 63.12 mS cm^{-1} at 70 °C. The membranes were stable and showed slow degradation in 1 M carbonate solution (pH 11) compared to 1 M hydroxide solution (pH > 14) at 50 °C.

The availability of solubilized AEM ionomer enables the use of conventional ink electrode fabrication techniques. Low temperature carbonate fuel cells using these AEMs operating on $H_2/O_2 + CO_2$ were demonstrated. The maximum power density was 4.1 mW cm^{-2} which was an order of magnitude greater than our

previous report using a commercial AEM. Results show the involvement of carbonate in the cycle (CO_2 consumption at the cathode and generation at the anode) in operating cell.

References

[1] J. Weber, K.D. Kreuer, J. Maier, A. Thomas, Adv. Mater. 20 (2008) 2595–2598.
[2] M.P. Nieh, M.D. Guiver, D.S. Kim, J.F. Ding, T. Norsten, Macromolecules 41 (2008) 6176–6182.
[3] P.C. Su, C.C. Chao, J.H. Shim, R. Fasching, F.B. Prinz, Nano Lett. 8 (2008) 2289–2292.
[4] J.H. Chen, M. Asano, Y. Maekawa, M. Yoshida, J. Polym. Sci. Polym. Chem. 46 (2008) 5559–5567.
[5] D.S. Kim, Kim YS), M.D. Guiver, B.S. Pivovar, J. Membrane. Sci. 321 (2008) 199–208.
[6] P. Jain, L.T. Biegler, M.S. Jhon, AIChE J. (2008) 2089–2100.
[7] Y.Z. Fan, H.Q. Hu, H. Liu, J. Power Sources 171 (2007) 348–354.
[8] H. Meng, M. Wu, X.X. Xu, M. Nei, Z.D. Wei, P.K. Shen, Fuel Cells 6 (2006) 447–450.
[9] E.H. Yu, K. Scott, J. Power Sources 137 (2004) 248–256.
[10] P. Zegers, J. Power Scoures 154 (2006) 497–502.
[11] J.H. Wee, K.Y. Lee, J. Power Scoures 157 (2006) 128–135.
[12] V. Rao, Hariyanto, C. Cremers, U. Stimming, Fuel Cells 5 (2007) 417–423.
[13] J.R. Varcoe, R.C.T. Slade, E. Lam How Yee, S.D. Poynton, D.J. Driscoll, D.C. Apperley, Chem. Mater. 19 (2007) 2686.
[14] J.R. Varcoe, R.C.T. Slade, E. Lam How Yee, Chem. Commun. (2006) 1428.
[15] K. Matsuoka, S. Chiba, Y. Iriyama, T. Abe, M. Matsuoka, K. Kikuchi, Z. Ogumi, Thin Solid Films 516 (2008) 3309–3313.
[16] L. Wu, T.W. Xu, D. Wu, X. Zheng, J. Membr. Sci. 310 (2008) 577–585.
[17] F. Yi, X. Yang, Y. Li, S. Fang, Polym. Adv. Technol. 10 (1999) 473–475.
[18] L. Li, Y.X. Wang, J. Membr. Sci. 262 (2005) 1.
[19] R.C.T. Slade, J.R. Varcoe, Solid State Ionics 176 (2005) 585.
[20] Y. Xiong, J. Fang, Q.H. Zeng, Q.L. Liu, J. Membr. Sci. 311 (2008) 319–325.
[21] J. Fang, P.K. Shen, J. Membr. Sci. 285 (2006) 317.
[22] T.S. Olson, E.E. Switzer, P. Atanassov, M.R. Hibbs, CJ. Cornelius. 211th ECS Meeting, Abstract #282.
[23] B.R. Einsla, E. McGrath, J. Am. Chem. Soc., Div. Fuel Chem. 49 (2004) 616–618.
[24] B. Lafitte, M. Puchner, P. Jannasch, Macromol. Rapid Commun. 26 (2005) 1464–1468.
[25] D.S. Kim, Y.S. Kim, M.D. Guiver, J.F. Ding, B.S. Pivovar, J. Power Sources 182 (2008) 100–105.
[26] S. Chempath, B.R. Einsla, L.R. Pratt, C.S. Macomber, J.M. Boncella, J.A. Rau, B.S. Pivovar, J. Phys. Chem. C 112 (2008) 3179–3182.
[27] J.S. Park, S.H. Park, S.D. Yim, Y.G. Yoon, W.Y. Lee, C.S. Kim, J. Power Sources 178 (2008) 620–626.
[28] K. Miyatake, Y. Chikashige, E. Higuchi, M. Watanabe, J. Am. Chem. Soc. 129 (13) (2007) 3879–3887.
[29] Y. Chikashige, Y. Chikyu, K. Miyatake, M. Watanabe, Macromolecules 38 (16) (2005) 7121–7126.
[30] G.J. Hwang, H. Ohya, T. Nagai, J. Membr. Sci. 156 (1999) 61–65.
[31] B. Wang, W. Huang, X. Yang, J. Appl. Polym. Sci. 96 (2005) 2117–2131.
[32] E. Avram, M.A. Brebu, A. Warshawasky, C. Vasile, Polym. Degrad. Stabil. 69 (2000) 175–181.
[33] M. Yang, W. Lin, J. Polym. Res. 9 (2002) 61–67.
[34] H. Herman, R.C.T. Slade, J.R. Varcoe, J. Membr. Sci. 218 (2003) 147–163.
[35] M.R. Hibbs, M.A. Hickner, T.M. Alam, S.K. McIntyre, C.H. Fujimoto, C.J. Cornelius, Chem. Mater. 20 (2008) 2566–2573.
[36] T.N. Danks, R.C.T. Slade, J.R. Varcoe, J. Mater. Chem. 13 (2003) 712–721.
[37] J.R. Varcoe, R.C.T. Slade, Fuel Cells 5 (2005) 187–200.
[38] Y.S. Kim, L. Dong, M.A. Hickner, T.E. Glass, V. Webb, J.E. McGrth, Macromolecules 36 (2003) 6281–6285.
[39] K. Miyatake, H. Zhou, H. Uchida, M. Watanabe, Chem. Commum. (2003) 368–369.
[40] R.C.T. Slade, J.R. Varcoe, Solid State Ionics 176 (5–6) (2005) 585–597.
[41] C.M. Lang, K. Kim, P.A. Kohl, Electrochem. Solid State 9 (2006) A545–A548.